Selective BD2 Inhibitor Exerts Anti-Fibrotic Effects via BRD4/FoxM1/Plk1 Axis in Orbital Fibroblasts From Patients With Thyroid Eye Disease

Yanyan Xie,[1] Yuan Pan,[1] Qian Chen,[1] Yuxi Chen,[1] Guanyu Chen,[1] Mei Wang,[2] Peng Zeng,[2] Zhuang Li,[1] Zuoyi Li,[1] Sha Wang,[3–5] Huasheng Yang,[1] and Dan Liang[1]

[1]Department of Ocular Immunology, State Key Laboratory of Ophthalmology, Zhongshan Ophthalmic Center, Sun Yat-Sen University, Guangzhou, China
[2]Department of Ophthalmology, Sun Yat-Sen Memorial Hospital, Sun Yat-Sen University, Guangzhou, China
[3]National Clinical Research Center for Geriatric Disorders, Xiangya Hospital, Central South University, Changsha, China
[4]Eye Center of Xiangya Hospital, Central South University, Changsha, China
[5]Hunan Key Laboratory of Ophthalmology, Changsha, China

Correspondence: Sha Wang, National Clinical Research Center for Geriatric Disorders, Xiangya Hospital, Central South University, Changsha 410008, China; wangsha_1982@csu.edu.cn. Huasheng Yang and Dan Liang, Department of Ocular Immunology, State Key Laboratory of Ophthalmology, Zhongshan Ophthalmic Center, Sun Yat-Sen University, Guangzhou 510060, China; yanghuasheng@gzzoc.com and liangdan@gzzoc.com.

YX and YP contributed equally to this work and share first authorship.

Received: January 31, 2023
Accepted: April 19, 2023
Published: June 5, 2023

Citation: Xie Y, Pan Y, Chen Q, et al. Selective BD2 inhibitor exerts anti-fibrotic effects via BRD4/FoxM1/Plk1 axis in orbital fibroblasts from patients with thyroid eye disease. *Invest Ophthalmol Vis Sci.* 2023;64(7):9. https://doi.org/10.1167/iovs.64.7.9

Purpose. We investigated the therapeutic potential of ABBV744, a bromodomain and extra-terminal (BET) inhibitor with selectivity for the second bromodomain (BD2) in thyroid eye disease (TED). The anti-fibrotic effects of ABBV744 and its underlying mechanism were explored in cultured orbital fibroblasts (OFs) from patients with TED.

Methods. Immunohistochemistry (IHC) and real-time quantitative polymerase chain reaction (RT-qPCR) assays were conducted on orbital connective tissues from TED and controls. RT-qPCR, Western blot, Cell-counting Kit-8 (CCK-8), and 5-ethynyl-2′-deoxyuridine (EdU) cell proliferation assays were conducted on OFs isolated from patients with TED.

Results. The expression of BRD4 was upregulated in the orbital tissues of patients with TED relative to controls and in TED OFs stimulated with TGF-β1. Further, we showed that BRD4 modulated the profibrotic process through the interaction with Forkhead Box M1 (FoxM1) and its downstream molecule Polo-like kinase 1 (Plk1) in cultured TED OFs. Inhibition of BRD4 both by BD2 selective inhibitor ABBV744 and pan-BET inhibitor JQ1 exerted anti-fibrotic effects, whereas ABBV744 displayed superior anti-fibrotic effects and acceptable safety compared to JQ1.

Conclusions. We conclude that BDR4 may modulate the profibrotic process in OFs of patients with TED via the FoxM1/Plk1 axis, and that selectively targeting BD2 domain of BRD4 may therefore be a potential therapeutic option for treating patients with TED.

Keywords: BRD4, BD2 selective inhibitor, thyroid eye disease (TED), fibrosis, orbital fibroblasts

Thyroid eye disease (TED), also known as Graves' ophthalmopathy (GO), is an organ-specific autoimmune disease that has disastrous effects on patients' appearance, vision, and quality of life. It occurs in approximately 50% of patients with Graves' disease (GD).[1,2] Currently, the main therapeutic strategies for TED, such as corticosteroids, orbital irradiation, and surgical decompression, still have difficulties to achieve desired outcome for the treatment of TED.[3–5] Finding a brand-new therapeutic target of TED is apparently in great demand.

However, the mechanisms involved in the pathogenesis of TED remain unclear. Orbital fibroblasts (OFs) are considered to be both target cells and pivotal effector cells in TED pathogenesis.[6,7] Fibrosis is the predominant pathologic feature in the late phase of TED, in which the excessive accumulation of extracellular matrix (ECM) resulted in increased expression of both alpha-smooth muscle actin (α-SMA) and collagen. This process eventually contributes to orbital tissue remodeling with extraocular muscle thickening and orbital volume expansion,[8] resulting in exophthalmos, eyelid and conjunctival swelling, limited ocular movements, and even compression of the optic nerve.[9] Unfortunately, despite the well-accepted role of fibrosis in the pathogenesis of TED, the initial triggers that promote the fibrotic process are unknown and few targeted anti-fibrotic drugs for TED exist.

Copyright 2023 The Authors

This work is licensed under a Creative Commons Attribution-NonCommercial-NoDerivatives 4.0 International License.

Downloaded from abstracts.iovs.org on 04/19/2024

The bromodomain (BD) and extra-terminal (BET) families are epigenetic readers that bind acetylated histones through their bromodomains to regulate gene transcription.[10,11] Members of the BET family include BRD2, BRD3, BRD4, and BRDT, which share in common a structure with two tandem BDs, called BD1 and BD2.[12,13] Recently, breakthrough progresses have been made to distinguish BD1 and BD2 functions in the pathogenesis of different diseases.[14–16] Among all BET members, most studies focus on BRD4, which plays a role in tumorigenesis by regulating gene expression.[17] BRD4 also activates hepatic stellate cells (HSCs) into myofibroblasts and contributes to liver fibrosis.[18] In addition, BRD4 controls the activation of cardiac fibroblasts and regulates cardiac fibrosis.[19,20] In TED, the persistent activation of OFs can result in devastating orbital fibrosis. It is worthwhile to determine the role of BRD4 in this pathologic fibrosis and its therapeutic potential.

It has been reported that inhibiting BRD4 could reverse pulmonary arterial hypertension,[21] potentially through interactions with Forkhead Box M1 (FoxM1) and Polo-like kinase 1 (Plk1) in microvascular endothelial cells and smooth muscle cells.[22] FoxM1 is a transcription factor known as a master regulator of cell cycle progression, and Plk1 is activated downstream by FoxM1.[23,24] Recent studies have shown that FoxM1 is a driver of lung fibroblast activation and that it increases the epithelial-to-mesenchymal transition (EMT) during radiation-induced pulmonary fibrosis.[25] These relationships raise the question of whether targeting BRD4 could have anti-fibrotic effects via FoxM1/Plk1 axis in TED.

JQ1, a pan-BET inhibitor which have similar affinities to BD1 and BD2 domains, can potently inhibit cardiac fibroblast activation and block cardiac fibrosis in mice.[26–28] However, common adverse effects of pan-BET inhibitors in clinical trials, such as thrombocytopenia, greatly limit their further therapeutic application.[29,30] Strikingly, inhibitors selectively targeting one particular BD domain have been found to display different efficacy and tolerability profile compared with pan-BET inhibitors. More specifically, inhibitors targeting the BD1 domain phenocopy the effects of pan-BET inhibitors in cancers, whereas BD2 selective inhibitors are crucially effective in immune-inflammatory diseases.[31] ABBV744, a highly potent and selective inhibitor with 290 times stronger affinity for BD2 than BD1, displays antiproliferative activity in tumor cell lines and shows fewer platelet and gastrointestinal toxicities than the pan-BET inhibitor ABBV-075.[32] Therefore, we hypothesize that ABBV744, as a highly selective BD2 inhibitor, might achieve an excellent therapeutic index with good tolerability in patients with TED.

Collectively, our aim is to determine whether ABBV744, a selective BET inhibitor targeting the BD2 domain of BRD4, could exert anti-fibrotic effects with better safety than pan-BET inhibitor, JQ1, via downregulation of the BRD4/FoxM1/Plk1 axis.

Methods

Participant Enrollment and Bioinformatic Analysis

Orbital connective tissues were consecutively obtained from ten patients with TED who underwent orbital decompression surgery at Zhongshan Ophthalmic Center, Xiangya Hospital and Sun Yat-Sen Memorial Hospital. All patients were euthyroid for at least 3 months before surgery. Consecutive control orbital connective tissues were collected from six normal control (NC) patients without TED or other history of thyroid disease, and who underwent blepharoplasty at the same institution. The demographic and clinical characteristics of the participants are summarized in Table 1. The clinical activity and severity were graded according to the 7-item Clinical Activity Score (CAS) and European Group on Graves' orbitopathy (EUGOGO), respectively.[33] All patients signed informed consent forms. This study was conducted according to the Declaration of Helsinki and approved by the Institutional Review Board of Zhongshan Ophthalmic Center (2020KYPJ104).

Additional bioinformatic analysis was done using orbital connective tissue from the Gene Expression Omnibus (GEO) database (No. GSE58331), including the tissue from 35 patients with TED and 29 NC patients.

The orbital connective tissues from TED and NC patients were used to perform immunohistochemistry (IHC) and real-time quantitative polymerase chain reaction (RT-qPCR) assays. The OFs isolated from patients with TED were used to perform the in vitro experiments, which included RT-qPCR, Western blot, Cell-counting Kit-8 (CCK-8), and 5-ethynyl-2′-deoxyuridine (EdU) cell proliferation assays. Due to the limited size of each orbital connective tissue, samples for IHC and RT-qPCR of tissues were not included in the experiment conducted in OFs in vitro. Samples from both sexes were used without preference.

Table 1. Baseline Demographic and Clinical Characteristics of Patients With Thyroid Eye Disease and Normal Controls

	Patients With TED	NCs
Patients, *n*	10	6
Sex, M/F, *n*	6/4	3/3
Age, mean (SD), y	47.4 (12.0)	31.7 (0.9)
Age, range, y	23–66	19–45
Smoking history, *n*	2	0
Clinical Activity Score (CAS)[a], *n*		
Inactive	10	n/a
Active	0	n/a
Disease severity[b], *n*		
Mild	0	n/a
Moderate-to-severe	10	n/a
Sight-threatening	0	n/a
Duration of illness, median (range), mo	15 (5–48)	n/a
Thyroid function at diagnosis of TED, *n*		
Hyperthyroid	8	n/a
Hypothyroid	2	n/a
Euthyroid	0	n/a
Therapeutic history, *n*		
Thyroid surgery	1	n/a
Orbital irradiation	1	n/a
Steroid treatment	3	n/a

SD, standard deviation; y, years; mo, months; n/a, not applicable.
[a] Clinical activity of TED was graded according to 7-item CAS Clinical Activity Score (CAS), which ranges from 0 to 7, is based on the classical signs of acute inflammation (i.e., pain, redness, swelling, and impaired function), and allows discrimination between the active and inactive stages of the disease (CAS $\geq$ 3 = active; CAS $<$ 3 = inactive).
[b] Severity was defined according to the European Group on Graves' orbitopathy (EUGOGO) classification, which uses specific criteria to determine whether the severity is mild, moderate-to-severe, or sight-threatening.

Investigative Ophthalmology & Visual Science

Downloaded from abstracts.iovs.org on 04/19/2024

Cell Cultures and Treatment

Tissues obtained from surgery were cut into pieces approximately 1 mm × 1 mm after removal of adipose tissues and blood vessels, and placed in T25 flasks. About 2 mL DMEM-F12 containing 20% fetal bovine serum (FBS) and 0.1% penicillin and streptomycin (both from Gibco Laboratories, Grand Island, NY, USA) was added and incubated at 37°C in a 5% CO2 humidified incubator. The media were changed every 3 days, and primary OFs were harvested after cells grew to confluence and were digested with a 0.25% trypsin solution (Gibco Laboratories). The cells were then sub-cultured in 6 cm plastic culture plates in DMEM-F12 with antibiotics and 10% FBS. OFs between the third and eighth passages were used for the subsequent experiments. Each part of the following experiment was repeated in OFs from at least three consecutive and independent specimens.

TGF-β1 (PeproTech Inc., Cranbury, NJ, USA), thiostrepton, BI6727, JQ1, and ABBV744 (all from Selleck Chemicals, Houston, TX, USA) were used for cell treatment. The solvent of thiostrepton, BI6727, JQ1, and ABBV744 was dimethylsulfoxide (DMSO; MP Biomedicals, Irvine, CA, USA). Control experiments were performed using DMSO as vehicle only without the addition of drugs.

Cell Proliferation Assays

CCK-8 assays (Beyotime Biotechnology, Shanghai, China) were conducted to evaluate cell viability. OFs were cultured in 96-well plates and treated with various concentrations of thiostrepton and BI6727 separately, and the optical density (OD) value was measured at the indicated times. Cell proliferation was assessed using EdU Cell Proliferation Kits (Beyotime Biotechnology), and the procedure was reported in a previous study.[34]

Small Interfering RNA Knockdown

Upon reaching a cell confluence of 70%, OFs were transfected with a small interfering RNA (siRNA) for 24 hours or 48 hours with RNAi Max reagent (RiboBio Co., Guangzhou, China), after which the culture media were replaced with fresh media, with or without 10 ng/mL TGF-β1. At indicated time, cells were harvested for RNA or protein extraction.

RNA Isolation and RT-qPCR

Total RNA of orbital connective tissues and OFs was extracted using an RNA-Quick Purification Kit (Yishan Biotechnology, Shanghai, China). The cDNA was synthesized using a HiScript II Q RT SuperMix for RT-qPCR (Vazyme, Nanjing, China). RT-qPCR was performed on a Roche LightCycler 480 (Roche, Basel, Switzerland) with the ChamQ SYBR Color qPCR Master Mix (Vazyme, Nanjing, China). GAPDH was used for normalization of results. Table 2 displayed the gene-specific primer sequences for RT-qPCR.

Immunohistochemistry

Paraffin-embedded tissues were cut into 3-µm thick slices, and then dewaxing, rehydration, and antigen retrieval. The slices were placed in 3% H2O2 and incubated at room temperature for 25 minutes after 3 washes with phosphate-buffered saline (PBS). After another wash, the slices were blocked with 3% bovine serum albumin (BSA) in PBS for 30 minutes. The slices were first incubated with primary antibody against BRD4 and FoxM1 (both from Abcam, Cambridge, UK) overnight at 4°C and then incubated with a goat-anti-rabbit secondary antibody for 50 minutes, followed by visualization with 3, 3-diaminobenzidine (DAB). After counterstaining of cell nuclei with hematoxylin, sections were sealed with neutral gum.

Table 2. Primer Sequences of RT-qPCR

Genes	Sequences (5′–3′)
BRD4	Forward: CCGCAAGCTCCAGGATGTGTTCG
	Reverse: GGCCACAACCTTGGTGGGAGG
FoxM1	Forward: CTTCCTAGACCACCTGGAGC
	Reverse: AGCCCAGTCCATCAGAACTC
Plk1	Forward: ATTCCCAAGCACATCAACCC
	Reverse: GGAGACGGGCAGGGATATAG
α-SMA	Forward: CTCTGGACGCACAACTGGCATC
	Reverse: CACGCTCAGCAGTAGTAACGAAGG
COL1 A1	Forward: AAAGATGGACTCAACGGTCTC
	Reverse: CATCGTGAGCCTTCTCTTGAG
COL1 A2	Forward: CTGGACCTCCAGGTGTAAGC
	Reverse: TGGCTGAGTCTCAAGTCACG
HAS1	Forward: ATGGTGCTTCTGTCGCTCTA
	Reverse: CACTCTGGTTCATGGTGACTAG
HAS2	Forward: AAGAACAACTTCCACGAAAAGG
	Reverse: TACATAATCCACACTTCGTCCC
HAS3	Forward: TTATACAGCTTTTCTACCGGGG
	Reverse: CAGAAGGCTGGACATATAGAGG
GAPDH	Forward: GACAGTCAGCCGCATCTTCT
	Reverse: GCGCCCAATACGACCAAATC

Western Blot

OFs were harvested, washed twice with cold PBS, and then lysed with the use of a protein extraction kit (KeyGEN, Nanjing, China). The following procedures were performed as previously described.[35] Primary antibodies were anti-β-Tublin (#2148), anti-COL 1 (#E8F4L), anti-FoxM1 (#D12D5), and anti-Plk1 (#208G4; Cell Signaling Technology, Boston, MA, USA), and anti-BRD4 (#ab128874) and anti-α-SMA (#ab5694; Abcam, Cambridge, UK). The intensity of each band was calculated with ImageJ software and β-Tublin was used for normalization of results.

Statistical Analysis

All experiments were performed using cell cultures isolated from at least three and up to five different patients with TED. Bioinformatics analyses were performed in R language using the Wilcoxon test. Data were analyzed using the Mann-Whitney U test or 1-way ANOVA. Results are presented as means with standard deviations and were calculated from three repeated experiments on each cell culture specimen. A P value < 0.05 was considered to indicate a statistically significant difference. All calculations and statistical analyses were performed using GraphPad Prism version 9 (GraphPad Software, Inc., La Jolla, CA, USA).

Results

BRD4 Expression is Upregulated in TED

Bioinformatics analysis from the GEO database showed significant upregulation of BRD4 in the orbital connective

Downloaded from abstracts.iovs.org on 04/19/2024

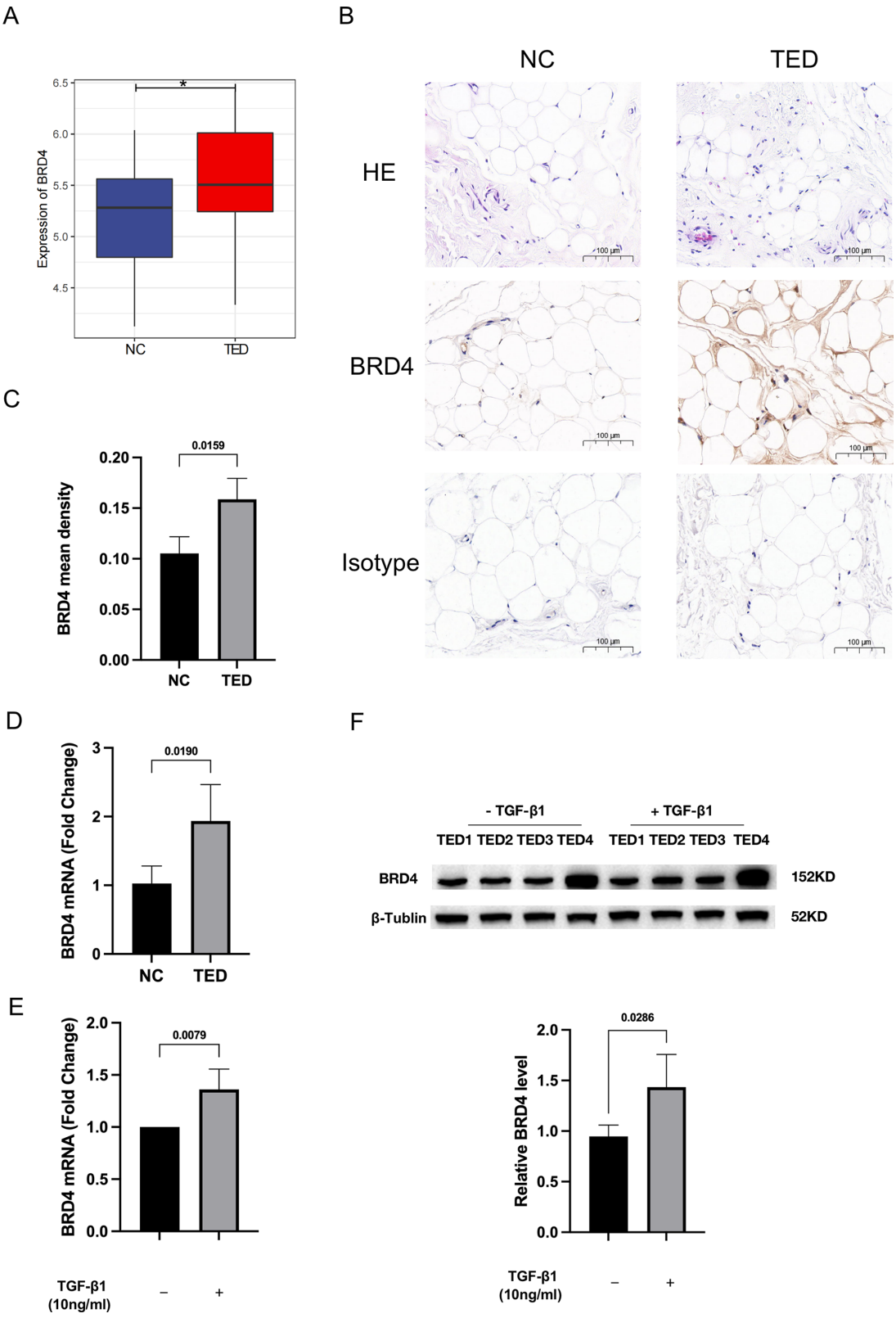

Figure 1. BRD4 levels in the orbital connective tissues and OFs. (**A**) Boxplot shows BDR4 expression in orbital connective tissues of the patients with TED ($n = 35$) and the NCs ($n = 29$) from GEO database No. GSE58331 ($P = 0.01$, analyzed by Wilcoxon test). (**B**) IHC staining for BRD4 (*yellow-brown*) was performed on biopsy sections of orbital connective tissues, and a representative staining for patients in the TED and NC groups is shown. Scale bar = 100 μm. (**C**) The mean density of BRD4 was used for the semiquantitative analysis of IHC. (**D**) RT-qPCR analysis shows BRD4 mRNA expression in consecutive orbital connective tissues from patients with TED ($n = 6$) and NCs ($n = 4$). (**E**) RT-qPCR analysis shows BRD4 mRNA expression in OFs of patients with TED ($n = 5$), after treatment for 24 hours with or without the fibrosis inducer TGF-β1. (**F**) Western blot analysis shows BRD4 protein expression (normalized to β-Tublin) in OFs of 4 consecutive patients with TED, treated for 48 hours with or without TGF-β1. Data are expressed as means ± SD; P values are displayed and $P < 0.05$ indicates a statistically significant difference.

Investigative Ophthalmology & Visual Science

Downloaded from abstracts.iovs.org on 04/19/2024

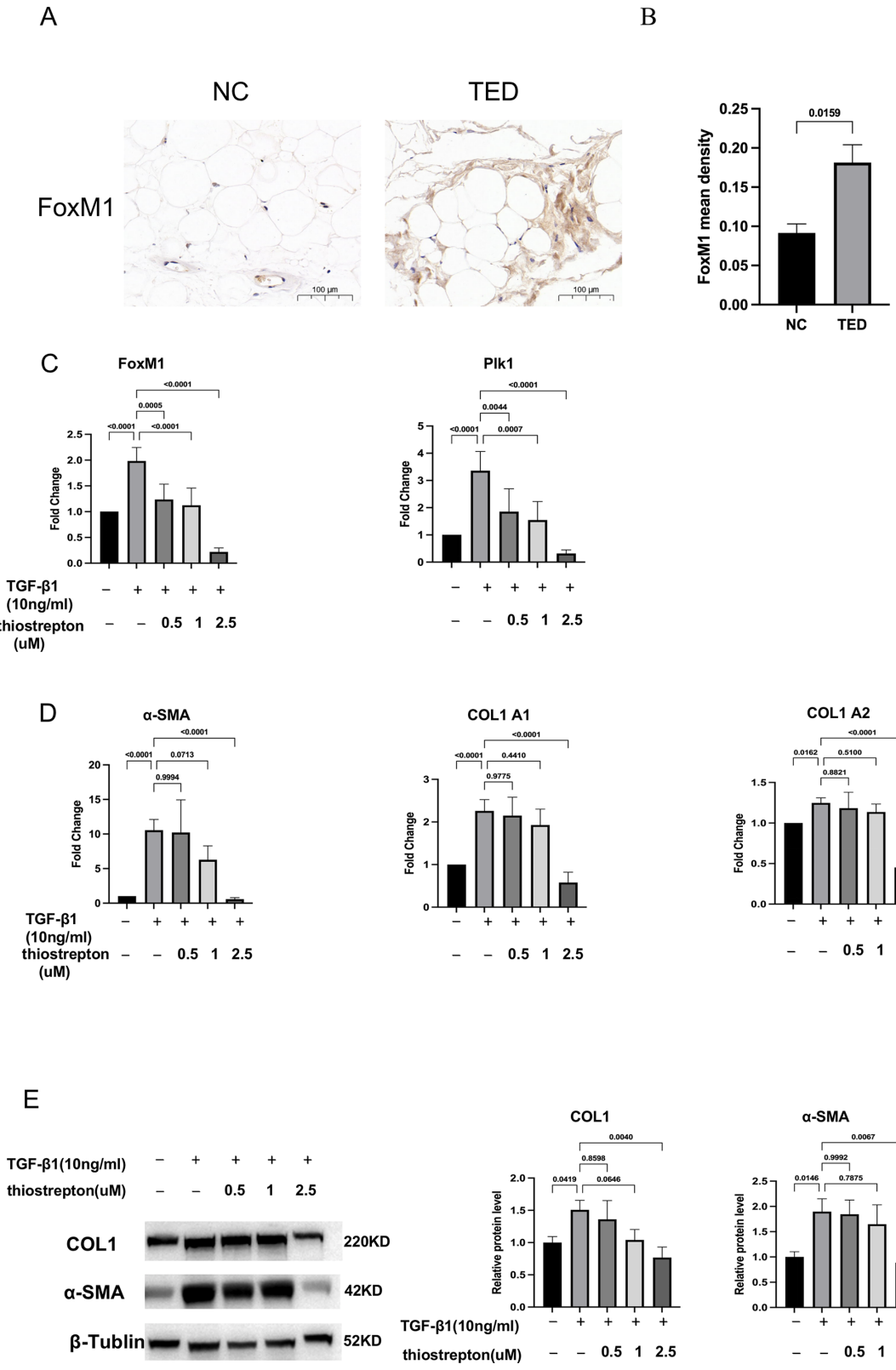

Figure 2. FoxM1 inhibition reduces fibrosis of the orbital tissue in TED. (**A**) IHC staining done for FoxM1 (*yellow-brown*) performed on biopsy sections of orbital connective tissue, and a representative staining for biopsies for patients in the TED and NC groups is shown. Scale bar = 100 μm. (**B**) The mean density of FoxM1 was used for the semiquantitative analysis of IHC. (**C, D**) Confluent OFs of patients with TED ($n = 5$) were left untreated or pretreated for 24 hours with different concentrations of the FoxM1 inhibitor thiostrepton (0.5, 1, or 2.5 uM) and then treated for 24 hours with or without the fibrosis inducer TGF-β1; subsequent RT-qPCR analysis shows mRNA levels of (**C**) FoxM1 and Plk1, and of (**D**) α-SMA, COL1 A1, and COL1 A2. (**E**) Western blot analysis shows protein expression of COL1 and α-SMA (normalized to β-Tublin) in OFs of patients with TED ($n = 3$), with or without exposure to thiostrepton (0.5, 1, or 2.5 uM), and treated for 48 hours with or without TGF-β1. Data are expressed as means ± SD; P values are displayed and $P < 0.05$ indicates a statistically significant difference.

Investigative Ophthalmology & Visual Science

Downloaded from abstracts.iovs.org on 04/19/2024

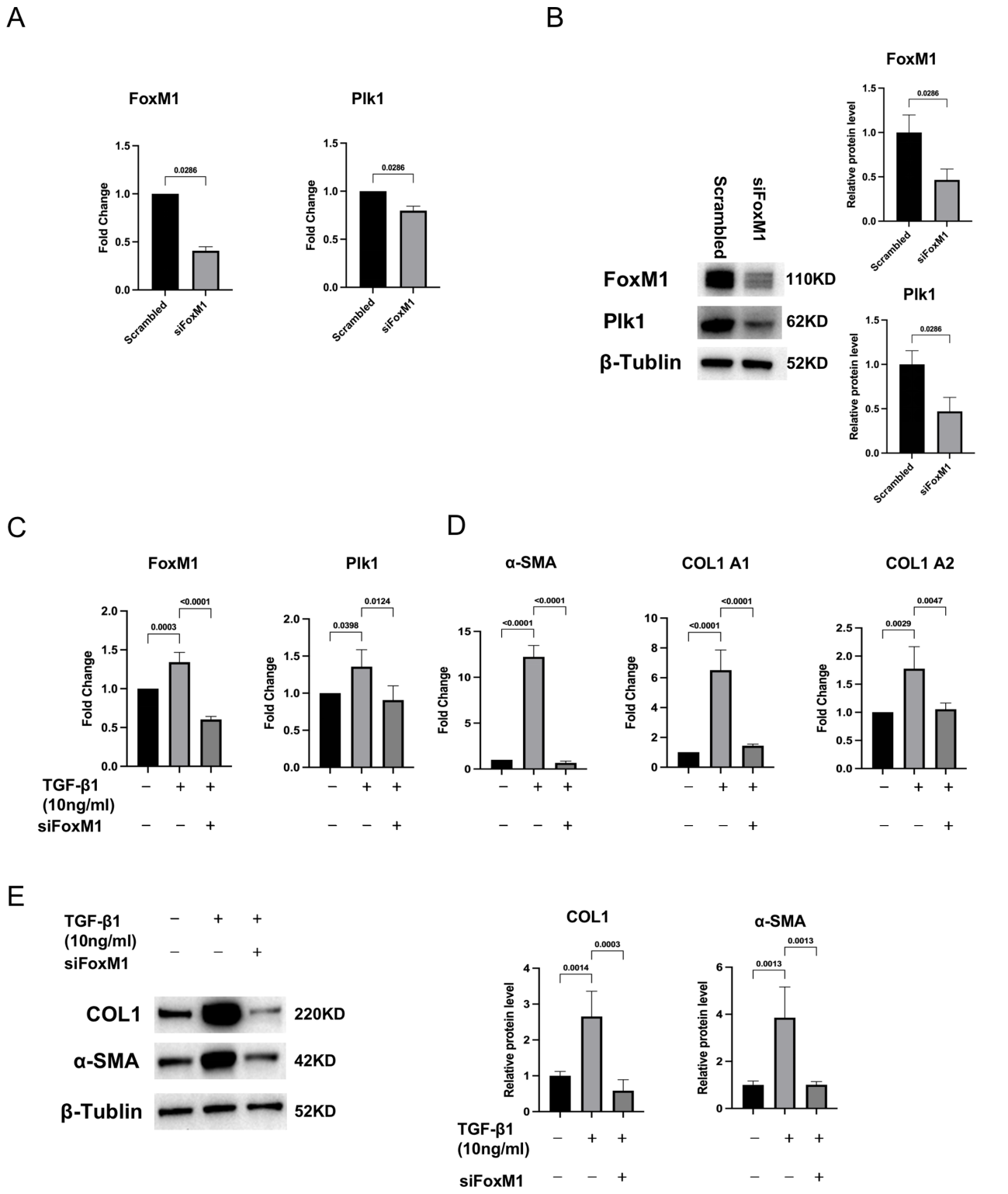

Figure 3. The siRNA knockdown of FoxM1 inhibits the orbital fibrosis of TED. (**A**) RT-qPCR quantification of FoxM1 and Plk1 mRNA knockdown efficiency by FoxM1-specific siRNA was performed on OFs from patients with TED ($n = 4$). (**B**) Western blot (normalized to β-Tublin) of FoxM1 and Plk1 protein knockdown efficiency by FoxM1-specific siRNA was done on OFs from patients with TED ($n = 4$). (**C, D**) RT-qPCR quantification of FoxM1-specific siRNA reduction of TGF-β1-induced increases in the mRNA expressions of **C** FoxM1 and Plk1, and of **D** α-SMA, COL1 A1, and COL1 A2, was performed on OFs from patients with TED ($n = 4$). (**E**) Western blot (normalized to β-Tublin) was done of FoxM1-specific siRNA reduction of TGF-β1-induced increases in the protein expressions of α-SMA and COL1 in OFs from patients with TED ($n = 4$). Data are expressed as means ± SD; P values are displayed and $P < 0.05$ indicates a statistically significant difference.

Investigative Ophthalmology & Visual Science

Downloaded from abstracts.iovs.org on 04/19/2024

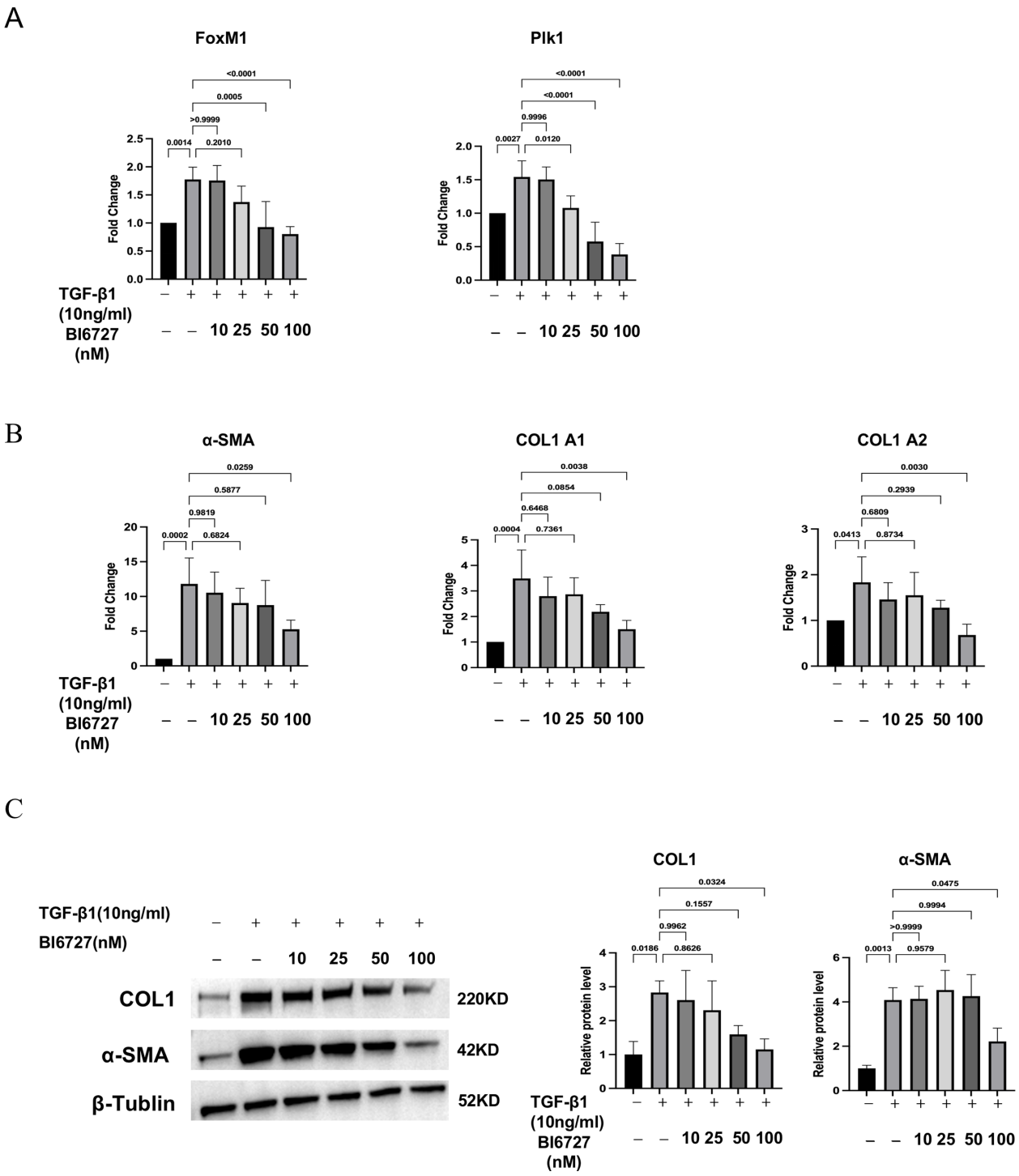

Figure 4. PLK1 inhibition ameliorates the orbital fibrosis of TED. (**A**) and (**B**) Confluent OFs of patients with TED ($n = 4$) were left untreated or pretreated for 24 hours with different concentrations of the Plk1 inhibitor BI6727 (10, 25, 50, or 100 nM) and then treated for 24 hours with or without TGF-β1; subsequent RT-qPCR analysis shows mRNA levels of **A** FoxM1 and Plk1, and of **B** α-SMA, COL1 A1, and COL1 A2. (**C**) Western blot analysis shows protein expression (normalized to β-Tublin) of COL1 and α-SMA in OFs of patients with TED ($n = 3$), with or without exposure to BI6727 (10, 25, 50, or 100 nM), and treated for 48 hours with or without TGF-β1. Data are expressed as means ± SD; P values are displayed and $P < 0.05$ indicates a statistically significant difference.

tissues of patients with TED relative to NCs (Fig. 1A). IHC showed BRD4 immunoreactivity was stronger in patients with TED than in NCs (Figs. 1B, 1C). In addition, mRNA expression of BRD4 in orbital connective tissues was significantly higher in patients with TED than in NCs (Fig. 1D). Next, we used a TGF-β1-induced profibrotic model in vitro to further confirm upregulation of BRD4 in TED OFs, we observed that mRNA (Fig. 1E) and protein (Fig. 1F) expression of BRD4 in TED OFs after TGF-β1 stimulation both increased.

Investigative Ophthalmology & Visual Science

Downloaded from abstracts.iovs.org on 04/19/2024

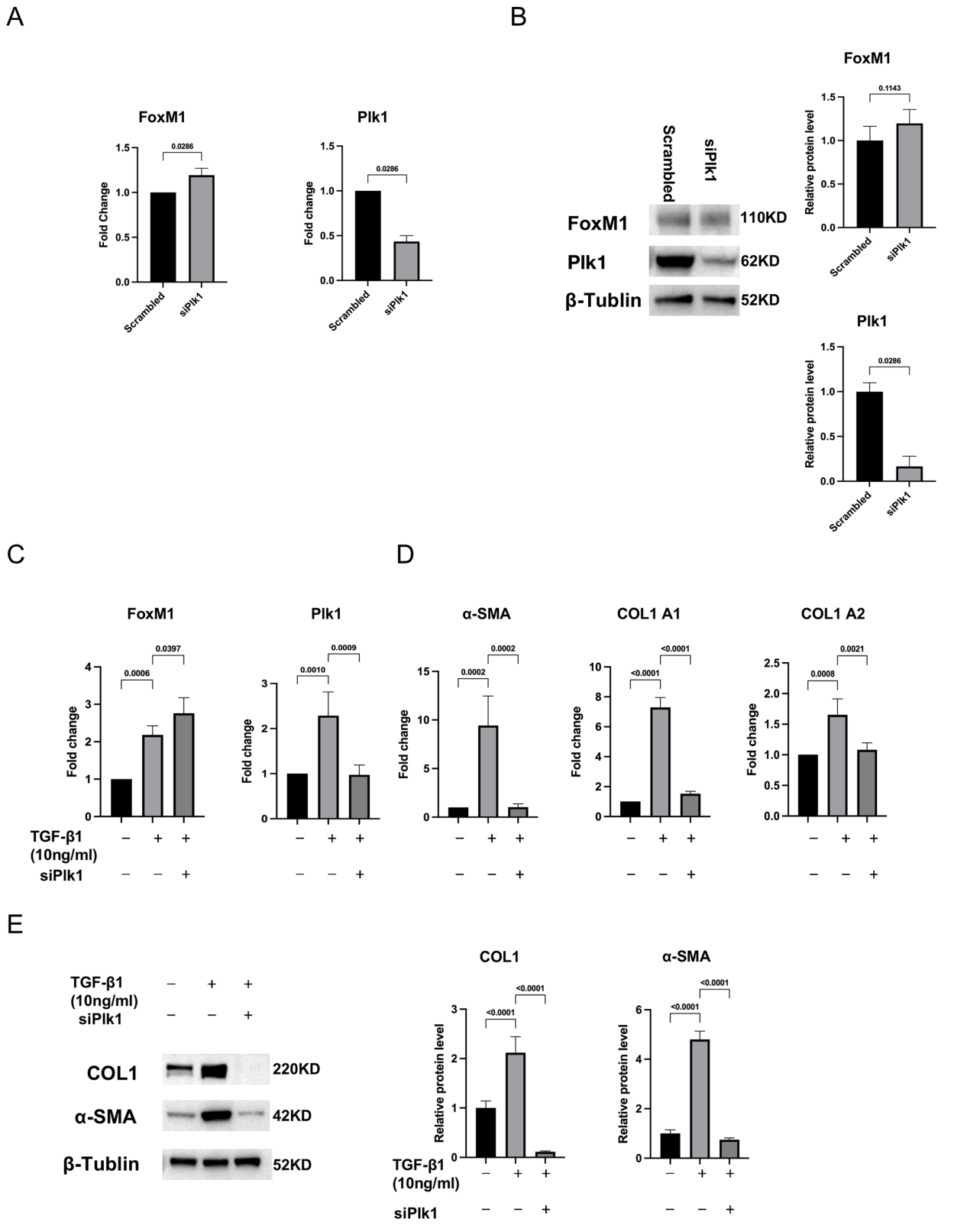

Figure 5. The siRNA knockdown of Plk1 attenuates the orbital fibrosis of TED. (**A**) RT-qPCR quantification of FoxM1 and Plk1 mRNA knockdown efficiency by Plk1-specific siRNA was performed on OFs from patients with TED ($n = 4$). (**B**) Western blot (normalized to β-Tublin) of FoxM1 and Plk1 protein knockdown efficiency by Plk1-specific siRNA was done on OFs from patients with TED ($n = 4$). (**C**) and (**D**) RT-qPCR quantification of Plk1-specific siRNA reduction of TGF-β1-induced increases in the mRNA expressions of **C** FoxM1 and Plk1, and of **D** α-SMA, COL1 A1, and COL1 A2, was performed on OFs from patients with TED ($n = 4$). (**E**) Western blot (normalized to β-Tublin) was done of Plk1-specific siRNA reduction of TGF-β1-induced increases in the protein expressions of α-SMA and COL1 in OFs from patients with TED ($n = 4$). Data are expressed as means $\pm$ SD; P values are displayed and $P < 0.05$ indicates a statistically significant difference.

Investigative Ophthalmology & Visual Science

Downloaded from abstracts.iovs.org on 04/19/2024

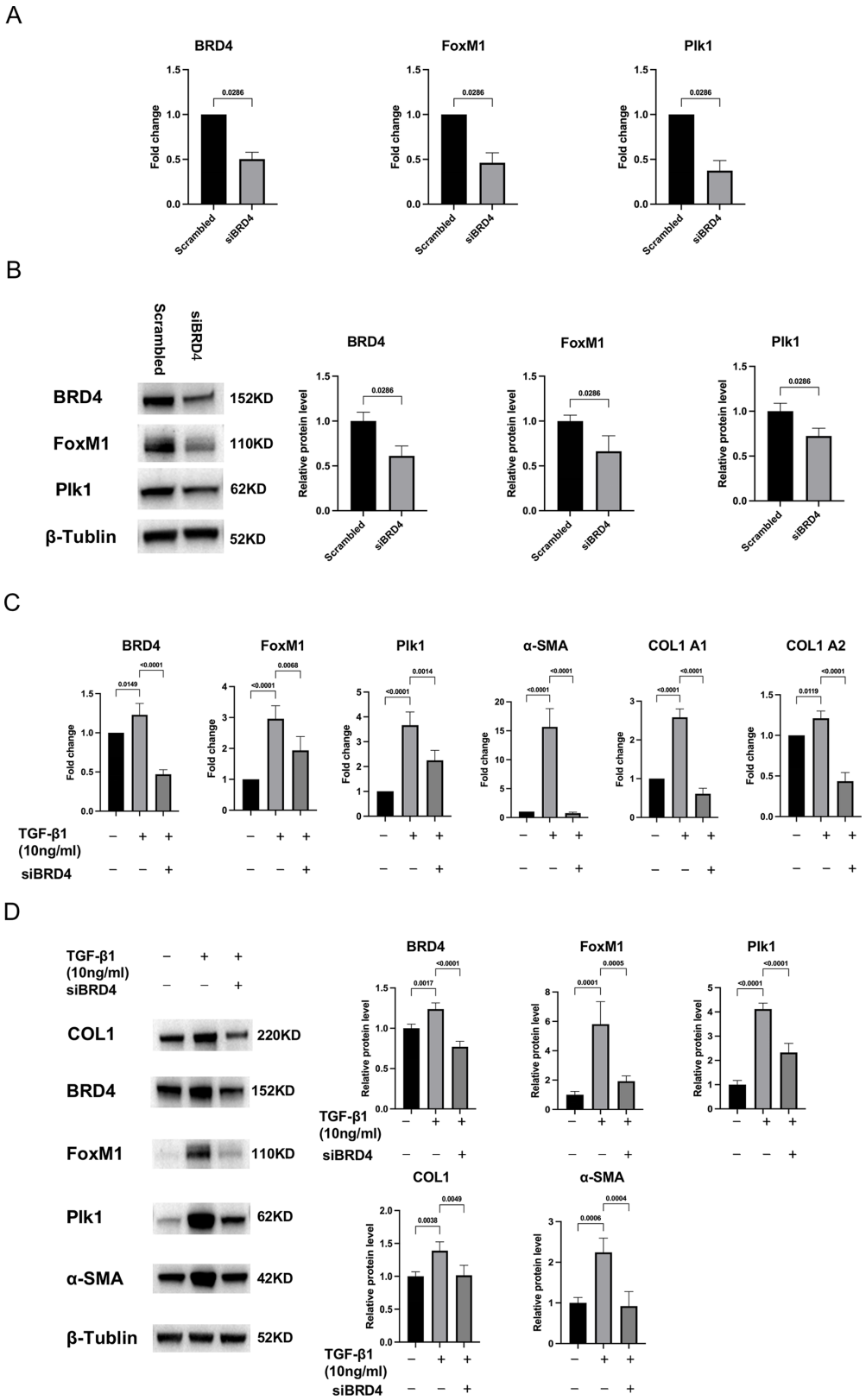

Figure 6. BRD4 regulates FoxM1/Plk1 pathway during the fibrosis of TED. (**A**) RT-qPCR quantification of BRD4, FoxM1, and Plk1 mRNA knockdown efficiency by BRD4-specific siRNA was performed on OFs from patients with TED ($n = 4$). (**B**) Western blot (normalized to β-Tublin) of BRD4, FoxM1, and Plk1 protein knockdown efficiency by BRD4-specific siRNA was done on OFs from patients with TED ($n = 4$). (**C**) RT-qPCR quantification of BRD4-specific siRNA reduction of TGF-β1-induced increases in the mRNA expressions of FoxM1, Plk1, α-SMA, COL1 A1, and COL1 A2 was performed on OFs from patients with TED ($n = 4$). (**D**) Western blot (normalized β-Tublin) was done of BRD4-specific siRNA reduction of TGF-β1-induced increases in the protein expressions of FoxM1, Plk1, α-SMA, and COL1 in OFs from patients with TED ($n = 4$). Data are expressed as means ± SD; P values are displayed and $P < 0.05$ indicates a statistically significant difference.

Investigative Ophthalmology & Visual Science

Downloaded from abstracts.iovs.org on 04/19/2024

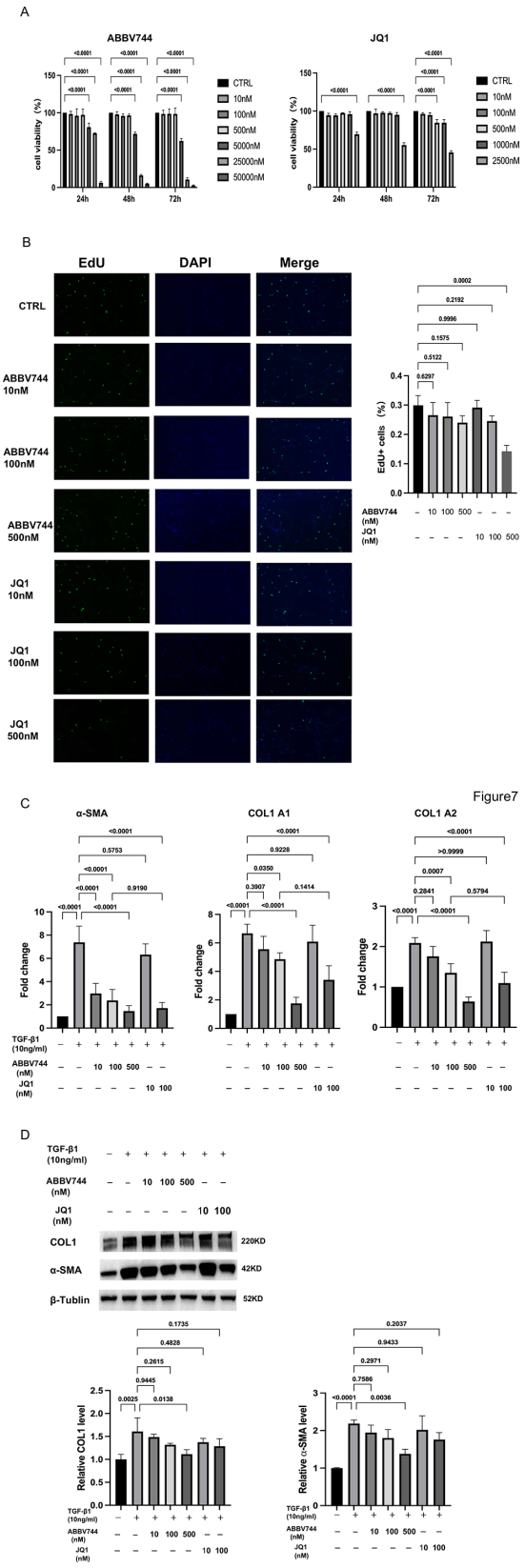

Figure 7. Selective BD2 inhibitor demonstrates better safety profile and anti-fibrotic effect than pan-BET inhibitor. (**A**) CCK-8 assays were done on OFs from patients with TED ($n = 3$) that were treated separately with various concentrations of the selective BD2 inhibitor ABBV744 (0, 10, 100, 500, 5000, 25,000, or 50,000 nM) or with various concentrations of the pan-BET inhibitor JQ1 (0, 10, 100, 500, 1000, or 2500 nM), each for 24, 48, or 72 hours; OF cell viability results are shown, calculated as a proportion of all viable untreated cells. (**B**) Representative images are shown of the results of EdU incorporation assays in OFs from patients with TED ($n = 4$) treated with ABBV744 (10, 100, or 500 nM) or JQ1 (10, 100, or 500 nM), and in untreated OF controls. Scale bar = 100 µm. Color scheme: *Green*, EdU; and *Blue*, DAPI. Histogram shows proportions of EdU positive cells. (**C, D**) Confluent OFs of patients with TED ($n = 4$) were left untreated or pretreated with ABBV744 (10, 100, or 500 nM) or JQ1 (10 or 100 nM) for 24 hours, and then either **C** treated with or without the fibrosis inducer TGF-β1 for 24 hours, after which RT-qPCR was used to measure the mRNA levels of α-SMA, COL1 A1, and COL1 A2, or **D** treated with or without TGF-β1 for 48 hours, after which Western blot (normalized to β-Tublin) was used to measure the protein expression of COL1 and α-SMA. Data are expressed as means ± SD; P values are displayed and $P < 0.05$ indicates a statistically significant difference.

FoxM1 is Involved in the Orbital Tissue Fibrosis of TED

FoxM1 is a key transcription factor mediating EMT in pulmonary fibrosis,[25] and we found that FoxM1 immunoreactivity was stronger in the orbital connective tissues of patients with TED than NCs (Figs. 2A, 2B). CCK-8 assays showed that concentrations of 0.5 uM, 1 uM, and 2.5 uM of a FoxM1 inhibitor, thiostrepton were safe for TED OFs (Supplementary Fig. S1A).

To determine the role of FoxM1 in the fibrotic process in vitro, we noted that TGF-β1 elicited a notable increase in the mRNA level of FoxM1, and its downstream molecule Plk1, and that thiostrepton diminished this effect in a dose-dependent manner (Fig. 2C), possibly implicating the involvement of FoxM1/Plk1 axis in TED fibrosis. Additionally, pretreatment with thiostrepton at a concentration of 2.5 uM prevented TGF-β1-induced fibrosis in vitro (Figs. 2D, 2E).

To confirm the vital role of FoxM1 in the fibrosis of TED, FoxM1-specific siRNA was used. We excluded the influence of scrambled siRNA and transfection reagents in transfection efficiency and the baseline effect of siFoxM1 on fibrosis related markers (Supplementary Figs. S2A, S2B, S2C, S2D). The siFoxM1 resulted in lower FoxM1 mRNA (Fig. 3A) and protein (Fig. 3B) expression than scrambled siRNA. Strikingly, siFoxM1 also reduced the TGF-β1-induced increases in expressions of FoxM1 and Plk1 (Fig. 3C), as well as fibrosis markers, in OFs (Fig. 3D). Western blot confirmed these results (Fig. 3E). Together, these findings implicate that FoxM1 is involved in the pathogenic fibrosis of TED, probably by mediating the downstream molecule Plk1.

PLK1 Inhibition Ameliorates the Orbital Fibrosis of TED

To validate the role of the FoxM1/Plk1 axis in TED fibrogenesis, we investigated whether Plk1 works with FoxM1 in modulating fibrosis in OFs. CCK-8 assays showed that concentrations of 10 nM, 25 nM, 50 nM, and 100 nM of BI6727, a Plk1 inhibitor were safe for OFs (see Supplementary Fig. S1B).

As we found above, FoxM1 and Plk1 mRNA levels were dramatically elevated after stimulation by TGF-β1, whereas BI6727 treatment significantly reduced FoxM1 and Plk1 mRNA expression at indicated concentrations (Fig. 4A). In addition, BI6727 of 100 nM significantly reduced expression

Investigative Ophthalmology & Visual Science

Downloaded from abstracts.iovs.org on 04/19/2024

of fibrosis-related markers that were increased by TGF-β1 stimulation in mRNA (Fig. 4B) and protein levels (Fig. 4C).

To better illustrate the role of Plk1 in the fibrosis of TED, we blocked Plk1 using siPlk1. We observed high knockdown efficiency of Plk1 at the gene and protein levels in the siPlk1-transfected OFs (Figs. 5A, 5B; see Supplementary Figs. S3A, S3B) and excluded the baseline effect of siPlk1 on fibrosis-related markers (see Supplementary Figs. S3C, S3D). In contrast, the FoxM1 mRNA level was a little higher, and the FoxM1 protein level was not significantly higher, in siPlk1-transfected OFs. Figure 5C showed that siPlk1 reduced the TGF-β1-induced increases in the expression of Plk1, but that it increased the expression of the FoxM1. In addition, we found that siPLK1 markedly reduced the indicators of TGF-β1-induced fibrosis at the transcription (Fig. 5D) and protein level (Fig. 5E). Taken together, these results provide evidence of the role of Plk1 in TED fibrosis.

BRD4 Regulates the FoxM1/Plk1 Axis During in the Profibrotic Process of TED

Whereas our previous results have implied that BRD4, FoxM1, and Plk1 are all involved in TED fibrosis, it is unknown whether BRD4 actually modulates fibrosis via the FoxM1/Plk1 axis. We found that siBRD4 significantly reduced the expression of BRD4, FoxM1, and Plk1 (Figs. 6A, 6B; Supplementary Figs. S4A, S4B) and siBRD4 had no baseline effect on fibrosis related markers (Supplementary Figs. S4C and S4D).

In addition, we found that siBRD4 dramatically undermined TGF-β1-induced increases in the expressions of BRD4, FoxM1, Plk1, and fibrosis-related markers at the mRNA (Fig. 6C) and protein level (Fig. 6D). Notably, we found that siBRD4 partially attenuated the accumulation of hyaluronan (HA) (Supplementary Fig. S5A). Taken together, these results provide evidence that BRD4 does modulate the activation of fibrogenesis in TED via the FoxM1/Plk1 axis.

ABBV744 Exerts Anti-Fibrotic Effects in TED

To further investigate whether targeting BRD4 might be therapeutic beneficial, the pan-BET inhibitor JQ1 and the selective BD2 inhibitor ABBV744 were applied. Figure 7A showed JQ1 and ABBV744 had minimal cytotoxicity at concentrations of $\leq$100 nM and $\leq$500 nM, respectively. Figure 7B demonstrated JQ1 of 500 nM significantly lowered the proportion of EdU-positive OFs whereas ABBV744 did not.

ABBV744 at all concentrations significantly reduced α-SMA mRNA expression in TGF-β1-induced OFs, whereas JQ1 exerted such effect only at 100 nM (Fig. 7C). In addition, ABBV744 at concentrations of 100 nM and 500 nM, and JQ1 at a concentration of 100 nM, reduced COL1 A1 and COL1A2 mRNA expressions. The mRNA expressions of fibrosis-related markers showed no statistically significant changes when treated with either ABBV744 or JQ1 of 100 nM.

In the protein levels, only ABBV744 of 500 nM exerted anti-fibrotic effects. (Fig. 7D). Taken together, our results imply that the selective BD2 inhibitor ABBV744 is superior to pan-BET inhibitor JQ1 considering safety profile and anti-fibrotic effect at the same concentrations. This suggests that targeting the BD2 domain of BRD4 may be a safe and effective therapeutic option to control the fibrosis of TED.

Discussion

In this report, we have provided evidence that BRD4 has a role in TED pathophysiology and modulates pathological fibrosis of TED via FoxM1/Plk1 axis. Most importantly, we showed that a selective inhibitor targeting the BD2 domain of BRD4 displayed promising anti-fibrotic effects in cultured TED OFs. Together, these results underscore the potential value of selectively targeting the BD2 domain of BRD4 in the treatment of TED fibrosis.

Fibrosis in vital organs may contribute to about 45% of deaths in developed countries, and studies have reported that BRD4 was involved with the development of fibrosis. It has been reported that BRD4 was required for the activation of HSCs (key effector cells in liver fibrosis) in response to TGF-β1 stimulation and JQ1 suppressed the proliferation and differentiation of HSCs into myofibroblasts in liver fibrosis.[18,36] Additionally, JQ1 could blunt the induction of α-SMA and COL1 A1 when stimulated by TGF-β1 in cultured lung fibroblasts (target cells in lung fibrosis).[37] However, little is known about BRD4 in the pathologic profibrotic process of TED. Our results shed some light, demonstrating that BRD4 was upregulated in both the orbital connective tissues and Ofs of patients with TED relative to controls and that the inhibition of BRD4 suppressed the profibrotic process in TED.

Studies have shown that BRD4 inhibitors reduced FoxM1 expression at both the transcriptional and protein levels in the smooth muscle cells isolated from patients with pulmonary arterial hypertension.[22,38] In addition, acting as a transcription factor, FoxM1 can induce the EMT in alveolar type II epithelial cells and activate lung fibroblast differentiation.[25,39] In this study, we have demonstrated that FoxM1 was upregulated in patients with TED. Furthermore, we have shown that FoxM1 expression was higher in the orbital connective tissues of patients with TED relative to controls, was substantially increased after the TGF-β1-induced stimulation of OFs, and was a stimulator of increases in the expressions of profibrotic genes in TED. We have also demonstrated that TGF-β1-induced upregulation of FoxM1 was significantly undermined by both a small molecule inhibitor of FoxM1 and a FoxM1-specific siRNA. These findings provide evidence that FoxM1 may play a critical role in the profibrotic process of TED.

Similarly, FoxM1 is known to regulate Plk1. Consistent with the fact that Plk1 is a well-characterized downstream effector of FoxM1,[22,23,40] we have shown in our study that inhibition of FoxM1 resulted in the decreased expression of Plk1. We have also demonstrated that inhibition of Plk1, with either BI6727 or Plk1-specific siRNA, exerted anti-fibrotic effects. Interestingly, we found that BI6727, a small molecule inhibitor of Plk1, downregulated FoxM1 mRNA expression while siPlk1 upregulated FoxM1 mRNA expression, which is a little bit different from a previous study that claims a positive feedback loop between FoxM1/Plk1 axis.[23] This difference may be because siRNA and small molecule inhibitors tend to target mRNA and protein expression, respectively. In brief, our results indicate that BRD4 may regulate the FoxM1/Plk1 axis in the profibrotic process of TED.

The pan-BET inhibitor JQ1 has been shown to alleviate fibrosis in other organs, such as the lungs, liver, kidneys, and skin explants from patients with systemic sclerosis.[18,28,37,41–43] Collectively, these data underscore the potential of BET inhibitors as strategies for management of fibrotic diseases. Indeed, BET inhibitors have shown

Investigative Ophthalmology & Visual Science

Downloaded from abstracts.iovs.org on 04/19/2024

broad and potent anticancer activity in preclinical studies.[44–48] Whereas, clinical studies of pan-BET inhibitors have reported modest oncologic efficacy but severe adverse events, including thrombocytopenia and gastrointestinal toxicity.[30] As an example, JQ1 has shown excellent therapeutic effects in multiple preclinical tumor models, but its side effects have limited its clinical application.[45] However, ABBV744, a BD2 selective inhibitor which is 100 times more selective for BD2 than BD1, has demonstrated better efficacy and tolerability than the pan-BET inhibitor ABBV-075.[49,50] ABBV744 is now the subject of 2 clinical trials (NCT03360006 and NCT04454658), the latter involving myelofibrosis. In our study, ABBV744 and JQ1 had similar anti-fibrotic effects at the mRNA level. In contrast, only ABBV744 reduced the expression of fibrosis-related markers at the protein level. These results are consistent with a previous study in a mouse xenograft model which showed that ABBV744 at 1/16 maximum tolerated dose (MTD) achieved superior anti-tumor activity to JQ1 at its full MTD.[49] Besides, ABBV744 demonstrated better safety than JQ1 at 500 nM. It has been reported that ABBV744 possesses half-maximum inhibitory concentrations (IC_{50}) of 2006 nM and 4 nM for the BD1 and BD2 domains of BRD4, respectively, compared to IC_{50} of 163 nM and 66 nM for JQ1.[49] Taken together, these results suggest that ABBV744 generates anti-fibrotic effects in a BD2-dependent manner with good safety, whereas JQ1 targets both the BD1 and BD2 domains and requires concentrations that are cytotoxic to OFs in order to exert its effects.

Previous studies have shown that BD2 selective inhibitors are capable of reducing hepatic fibrosis, and that BD2 inhibitors are predominantly effective in models of inflammatory and autoimmune disease than pan-BET inhibitors.[31] Our findings were consistent with those results, and we suggest that ABBA744 may be capable of reducing fibrosis in TED while generating less toxicity than pan-BET inhibitors. In turn, this suggests that targeting the BD2 domain may achieve favorable therapeutic index to address the progressive fibrotic process in TED.

Our study still has limitations. First of all, our experiments exclusively depended on an in vitro profibrotic model due to a lack of globally recognized mouse model of TED.[51] In addition, samples of the NC group were obtained from the eyelid, which might not perfectly match the biology function of TED groups obtained from the deep orbit. Besides, this study only concentrated on OFs and was short of the exploration of crosstalk between immunologically active cells and OFs or the influence of the microenvironment. Further in vivo exploration is needed to comprehensively elucidate the therapeutic potential of selective BD2 inhibitor in TED.

In conclusion, this study provides insights into the application of ABBV744, a BET inhibitor selectively targeting BD2 domain of BRD4, in the control of the profibrotic process of TED for the first time. Evidence is provided supporting a mechanism of TED in which BRD4 modulates the pathologic fibrosis via the FoxM1/Plk1 axis in cultured TED OFs. The results provide a rationale for pursuing clinical studies involving the selective BD2 inhibitor as a therapeutic strategy in patients with TED.

Acknowledgments

The authors appreciate Raymond K. Whalen, from Whalen Medical Communications, Professional Limited Liability Company for editing the English text of a draft of this manuscript. In addition, we appreciate all the participants in this study for selflessly offering samples to make this study possible.

Supported by funding from the Sun Yat-Sen University Clinical Research 5010 Program (2012015), the Science and Technological Planning Project of Guangzhou City (201704020051), the National Science and Technology Planning Project (2014BAI07B07), and the Natural Science Foundation of Hunan Province (2022JJ30964).

Disclosure: **Y. Xie**, None; **Y. Pan**, None; **Q. Chen**, None; **Y. Chen**, None; **G. Chen**, None; **M. Wang**, None; **P. Zeng**, None; **Z. Li**, None; **Z. Li**, None; **S. Wang**, None; **H. Yang**, None; **D. Liang**, None

References

1. Garrity JA, Bahn RS. Pathogenesis of Graves ophthalmopathy: implications for prediction, prevention, and treatment. *Am J Ophthalmol*. 2006;142:147–153.
2. Kang S, Hamed Azzam S, Minakaran N, Ezra DG. Rituximab for thyroid-associated ophthalmopathy. *Cochrane Database Syst Rev*. 2022;6:CD009226.
3. Wiersinga WM. Advances in treatment of active, moderate-to-severe Graves' ophthalmopathy. *Lancet Diabetes Endocrinol*. 2017;5:134–142.
4. Ruchala M, Sawicka-Gutaj N. Advances in the pharmacological treatment of Graves' orbitopathy. *Expert Rev Clin Pharmacol*. 2016;9:981–989.
5. Boboridis KG, Bunce C. Surgical orbital decompression for thyroid eye disease. *Cochrane Database Syst Rev*. 2011;12:CD007630.
6. Wang H, Atkins SJ, Fernando R, Wei RL, Smith TJ. Pentraxin-3 is a TSH-inducible protein in human fibrocytes and orbital fibroblasts. *Endocrinology*. 2015;156:4336–4344.
7. Woeller CF, Roztocil E, Hammond CL, Feldon SE, Phipps RP. The aryl hydrocarbon receptor and its ligands inhibit myofibroblast formation and activation: implications for thyroid eye disease. *Am J Pathol*. 2016;186:3189–3202.
8. Khong JJ, McNab AA, Ebeling PR, Craig JE, Selva D. Pathogenesis of thyroid eye disease: review and update on molecular mechanisms. *Br J Ophthalmol*. 2016;100:142–150.
9. Bartalena L, Baldeschi L, Boboridis K, et al. The 2016 European Thyroid Association/European Group on Graves' Orbitopathy Guidelines for the Management of Graves' Orbitopathy. *Eur Thyroid J*. 2016;5:9–26.
10. Cochran AG, Conery AR, Sims RJ, 3rd. Bromodomains: a new target class for drug development. *Nat Rev Drug Discov*. 2019;18:609–628.
11. Filippakopoulos P, Knapp S. Targeting bromodomains: epigenetic readers of lysine acetylation. *Nat Rev Drug Discov*. 2014;13:337–356.
12. Falkenberg KJ, Johnstone RW. Histone deacetylases and their inhibitors in cancer, neurological diseases and immune disorders. *Nat Rev Drug Discov*. 2014;13:673–691.
13. Shi J, Vakoc CR. The mechanisms behind the therapeutic activity of BET bromodomain inhibition. *Mol Cell*. 2014;54:728–736.
14. Gamsjaeger R, Webb SR, Lamonica JM, Billin A, Blobel GA, Mackay JP. Structural basis and specificity of acetylated transcription factor GATA1 recognition by BET family bromodomain protein Brd3. *Mol Cell Biol*. 2011;31:2632–2640.
15. Shi J, Wang Y, Zeng L, et al. Disrupting the interaction of BRD4 with diacetylated Twist suppresses tumorigenesis in basal-like breast cancer. *Cancer Cell*. 2014;25:210–225.
16. Lamonica JM, Deng W, Kadauke S, et al. Bromodomain protein Brd3 associates with acetylated GATA1 to promote its chromatin occupancy at erythroid target genes. *Proc Natl Acad Sci USA*. 2011;108:E159–E168.

Downloaded from abstracts.iovs.org on 04/19/2024

17. Hussong M, Kaehler C, Kerick M, et al. The bromodomain protein BRD4 regulates splicing during heat shock. *Nucleic Acids Res*. 2017;45:382–394.
18. Ding N, Hah N, Yu RT, et al. BRD4 is a novel therapeutic target for liver fibrosis. *Proc Natl Acad Sci USA*. 2015;112:15713–15718.
19. Stratton MS, Lin CY, Anand P, et al. Signal-dependent recruitment of BRD4 to cardiomyocyte super-enhancers is suppressed by a microRNA. *Cell Rep*. 2016;16:1366–1378.
20. Stratton MS, Bagchi RA, Felisbino MB, et al. Dynamic chromatin targeting of BRD4 stimulates cardiac fibroblast activation. *Circ Res*. 2019;125:662–677.
21. Meloche J, Potus F, Vaillancourt M, et al. Bromodomain-containing protein 4: the epigenetic origin of pulmonary arterial hypertension. *Circ Res*. 2015;117:525–535.
22. Van der Feen DE, Kurakula K, Tremblay E, et al. Multicenter preclinical validation of BET inhibition for the treatment of pulmonary arterial hypertension. *Am J Respir Crit Care Med*. 2019;200:910–920.
23. Fu Z, Malureanu L, Huang J, et al. Plk1-dependent phosphorylation of FoxM1 regulates a transcriptional programme required for mitotic progression. *Nat Cell Biol*. 2008;10:1076–1082.
24. Lam EW, Brosens JJ, Gomes AR, Koo CY. Forkhead box proteins: tuning forks for transcriptional harmony. *Nat Rev Cancer*. 2013;13:482–495.
25. Balli D, Ustiyan V, Zhang Y, et al. Foxm1 transcription factor is required for lung fibrosis and epithelial-to-mesenchymal transition. *EMBO J*. 2013;32:231–244.
26. Song S, Liu L, Yu Y, et al. Inhibition of BRD4 attenuates transverse aortic constriction- and TGF-beta-induced endothelial-mesenchymal transition and cardiac fibrosis. *J Mol Cell Cardiol*. 2019;127:83–96.
27. Anand P, Brown JD, Lin CY, et al. BET bromodomains mediate transcriptional pause release in heart failure. *Cell*. 2013;154:569–582.
28. Spiltoir JI, Stratton MS, Cavasin MA, et al. BET acetyl-lysine binding proteins control pathological cardiac hypertrophy. *J Mol Cell Cardiol*. 2013;63:175–179.
29. Cohen Aubart F, Emile JF, Carrat F, et al. Targeted therapies in 54 patients with Erdheim-Chester disease, including follow-up after interruption (the LOVE study). *Blood*. 2017;130:1377–1380.
30. Berthon C, Raffoux E, Thomas X, et al. Bromodomain inhibitor OTX015 in patients with acute leukaemia: a dose-escalation, phase 1 study. *Lancet Haematol*. 2016;3:e186–e195.
31. Gilan O, Rioja I, Knezevic K, et al. Selective targeting of BD1 and BD2 of the BET proteins in cancer and immunoinflammation. *Science*. 2020;368:387–394.
32. McDaniel KF, Wang L, Soltwedel T, et al. Discovery of N-(4-(2,4-Difluorophenoxy)-3-(6-methyl-7-oxo-6,7-dihydro-1H-pyrrolo[2,3-c]pyridin-4-yl)phenyl)ethanesulfonamide (ABBV-075/Mivebresib), a potent and orally available bromodomain and extraterminal domain (BET) family bromodomain inhibitor. *J Med Chem*. 2017;60:8369–8384.
33. Bartalena L, Kahaly GJ, Baldeschi L, et al. The 2021 European Group on Graves' orbitopathy (EUGOGO) clinical practice guidelines for the medical management of Graves' orbitopathy. *Eur J Endocrinol*. 2021;185:G43–G67.
34. Guo Y, Li H, Guan H, et al. Dermatopontin inhibits papillary thyroid cancer cell proliferation through MYC repression. *Mol Cell Endocrinol*. 2019;480:122–132.
35. Shi L, Ye H, Huang J, et al. IL-38 exerts anti-inflammatory and antifibrotic effects in thyroid-associated ophthalmopathy. *J Clin Endocrinol Metab*. 2021;106:e3125–e3142.
36. Hah N, Sherman MH, Yu RT, Downes M, Evans RM. Targeting transcriptional and epigenetic reprogramming in stromal cells in fibrosis and cancer. *Cold Spring Harb Symp Quant Biol*. 2015;80:249–255.
37. Tang X, Peng R, Ren Y, et al. BET bromodomain proteins mediate downstream signaling events following growth factor stimulation in human lung fibroblasts and are involved in bleomycin-induced pulmonary fibrosis. *Mol Pharmacol*. 2013;83:283–293.
38. Courboulin A, Paulin R, Giguere NJ, et al. Role for miR-204 in human pulmonary arterial hypertension. *J Exp Med*. 2011;208:535–548.
39. Penke LR, Speth JM, Dommeti VL, White ES, Bergin IL, Peters-Golden M. FOXM1 is a critical driver of lung fibroblast activation and fibrogenesis. *J Clin Invest*. 2018;128:2389–2405.
40. Shirakawa J, Tajima K, Okuyama T, et al. Luseogliflozin increases beta cell proliferation through humoral factors that activate an insulin receptor- and IGF-1 receptor-independent pathway. *Diabetologia*. 2020;63:577–587.
41. Tian B, Zhao Y, Sun H, Zhang Y, Yang J, Brasier AR. BRD4 mediates NF-kappaB-dependent epithelial-mesenchymal transition and pulmonary fibrosis via transcriptional elongation. *Am J Physiol Lung Cell Mol Physiol*. 2016;311:L1183–L1201.
42. Zhou B, Mu J, Gong Y, et al. Brd4 inhibition attenuates unilateral ureteral obstruction-induced fibrosis by blocking TGF-beta-mediated Nox4 expression. *Redox Biol*. 2017;11:390–402.
43. Shin JY, Beckett JD, Bagirzadeh R, et al. Epigenetic activation and memory at a TGFB2 enhancer in systemic sclerosis. *Sci Transl Med*. 2019;11:eaaw0790.
44. Dawson MA, Prinjha RK, Dittmann A, et al. Inhibition of BET recruitment to chromatin as an effective treatment for MLL-fusion leukaemia. *Nature*. 2011;478:529–533.
45. Filippakopoulos P, Qi J, Picaud S, et al. Selective inhibition of BET bromodomains. *Nature*. 2010;468:1067–1073.
46. Fish PV, Filippakopoulos P, Bish G, et al. Identification of a chemical probe for bromo and extra C-terminal bromodomain inhibition through optimization of a fragment-derived hit. *J Med Chem*. 2012;55:9831–9837.
47. Wyce A, Ganji G, Smitheman KN, et al. BET inhibition silences expression of MYCN and BCL2 and induces cytotoxicity in neuroblastoma tumor models. *PLoS One*. 2013;8:e72967.
48. Zuber J, Shi J, Wang E, et al. RNAi screen identifies Brd4 as a therapeutic target in acute myeloid leukaemia. *Nature*. 2011;478:524–528.
49. Faivre EJ, McDaniel KF, Albert DH, et al. Selective inhibition of the BD2 bromodomain of BET proteins in prostate cancer. *Nature*. 2020;578:306–310.
50. McDaniel KF, Wang L, Soltwedel T, et al. Discovery of N-(4-(2,4-Difluorophenoxy)-3-(6-methyl-7-oxo-6,7-dihydro-1H-pyrrolo[2,3-c]pyridin -4-yl)phenyl)ethanesulfonamide (ABBV-075/Mivebresib), a potent and orally available bromodomain and extraterminal domain (BET) family bromodomain inhibitor. *J Med Chem*. 2017;60:8369–8384.
51. Eckstein A, Philipp S, Goertz G, Banga JP, Berchner-Pfannschmidt U. Lessons from mouse models of Graves' disease. *Endocrine*. 2020;68:265–270.

Investigative Ophthalmology & Visual Science

Downloaded from abstracts.iovs.org on 04/19/2024